

Characterization and quantification of nanoparticle–antibody conjugates on cells using C₆₀ ToF SIMS in the event-by-event bombardment/detection mode

Li-Jung Chen^a, Sunny S. Shah^b, Jaime Silangcruz^b, Michael J. Eller^a, Stanislav V. Verkhoturov^a, Alexander Revzin^b, Emile A. Schweikert^{a,*}

^a Department of Chemistry, Texas A&M University, College Station, TX, USA

^b Department of Biomedical Engineering, University of California, Davis, CA, USA

ARTICLE INFO

Article history:

Received 15 October 2010

Received in revised form 4 January 2011

Accepted 8 January 2011

Available online 14 January 2011

Keywords:

Quantification of bioconjugations

Cell micropatterns

Biological surfaces

AuNPs–antiCD4 conjugates

Cluster SIMS

ABSTRACT

Cluster C₆₀ ToF-SIMS (time-of-flight secondary ion mass spectrometry) operated in the event-by-event bombardment-detection method has been applied to: (a) quantify the binding density of Au nanoparticles (AuNPs)–antiCD4 conjugates on the cell surface and (b) identify the binding sites between AuNPs and antibody. Briefly, our method consists of recording the secondary ions, SIs, individually emitted from a single C₆₀^{1,2+} impact. From the cumulative mass spectral data we selected events where a specific SI was detected. The selected records revealed the SIs co-ejected from the nanovolume impacted by an individual C₆₀ with an emission area of ~10 nm in diameter as an emission depth of 5–10 nm. The fractional coverage is obtained as the ratio of the effective number of projectile impacts on a specified sampling area (N_e) to the total number of impacts (N_o). In the negative ion mass spectrum, the palmitate (C₁₆H₃₁O₂⁻) and oleteate (C₁₈H₃₃O₂⁻) fatty acid ions present signals from lipid membrane of the cells. The signals at m/z 197 (Au⁻) and 223 (AuCN⁻) originate from the AuNPs labeled antibodies (antiCD4) bound to the cell surface antigens. The characteristic amino acid ions validate the presence of antiCD4. A coincidence mass spectrum extracted with ion at m/z 223 (AuCN⁻) reveals the presence of cysteine at m/z 120, documenting the closeness of cysteine and the AuNP. Their proximity suggests that the binding site for AuNP on the antibody is the sulfur-terminal cysteine. The fractional coverage of membrane lipid was determined to be ~23% of the cell surfaces while the AuNPs was found to be ~21%. The novel method can be implemented on smaller size NPs, it should thus be applicable for studies on size dependent binding of NP–antibody conjugates.

© 2011 Elsevier B.V. All rights reserved.

1. Introduction

Gold nanoparticles, AuNPs, are attractive for tagging biomolecules [1–6]. They are usually biocompatible and readily detectable with microscopic and chemical analysis techniques [3–7]. Nevertheless, boundaries are set to their detectability by their size and shape [5,7–9]. We present here a mass spectrometric method which provides enhanced information about the bonding of the NP, can determine the number of NPs in a given area of interest, and has the prospect of detecting NPs of dimension below those accessible by the scanning electron microscope (SEM). The mass spectrometric analysis uses ToF-SIMS with C₆₀ as projectiles. The experiments are run in the event-by-event bombardment/detection mode which allows to identify molecules co-located within a ~10 nm diameter, i.e., the emission area from an individual C₆₀ impact [10].

The novel capabilities are illustrated with the characterization of antibody–AuNP conjugates binding to immune cells. The test case involves anti-CD4 conjugated with AuNPs which are site-specific nanoprobe for recognizing CD4 antigen on surfaces of T-cells and monocytes [1,2,5,6,11–13]. Levels of CD4 antigen expression are particularly important in T-cells where this antigen provides an entry point for HIV [14–16]. To date AuNP–antiCD4 nanoprobe have been detected and localized by the transmission electron microscope (TEM) and the SEM. However, the instability of nanoparticle–biomolecule conjugates under the high electron dose of the TEM or SEM limits the microscopic detection [4,17,18].

SIMS in the event-by-event bombardment/detection mode offers the ability to detect the proximity of a nanoparticle probe to the amino acid sites of an antibody. In general, AuNPs are covalently or hydrophobically attached to the target antibody to site specifically label proteins. Cysteine, a sulfur-terminal amino acid, can form strong thiolate bonds with AuNPs. Schenkel and Wu utilized SIMS with coincidence counting to study the bonding of peptide and proteins and their non-covalent interactions [19]. We have previously reported a methodology to quantify the surface

* Corresponding author.

E-mail address: schweikert@mail.chem.tamu.edu (E.A. Schweikert).

coverage of Ag NPs on a glycine matrix and the surface coverage of micropatterned species [20–22]. The event-by-event bombardment/detection mode allows the identification of co-emitted SIs with an ion of interest. A coincidental ion mass spectrum can be obtained by summing all these coincidental events. The quantification of a surface fractional coverage has been determined in terms of the ratio of the number of effective impacts on a specimen (N_e) to the total numbers of primary ions sent to a target surface (N_0).

We demonstrate below the application of ToF-SIMS in the event-by-event bombardment/detection mode to: (a) evaluate the quantity of spherical NPs conjugated with antiCD4 attached on a cell [23] and (b) examine the binding sites between antibody molecules and NPs.

2. Materials and methods

2.1. Preparation of T-cell binding surfaces

2.1.1. Materials

3-Acryloxypropyl trichlorosilane was purchased from Gelest, Inc. (Morrisville, PA). 10× phosphate buffered saline (PBS) without calcium and magnesium was purchased from Sigma Aldrich (Saint Louis, MO). Formalin was purchased from Fischer Scientific. Purified mouse anti-human CD4 (13B8.2) was purchased from Beckman–Coulter (Fullerton, CA). Colloidal gold (30 nm) conjugated monoclonal antibody to human T-cell helper (AuNP/anti-CD4 conjugate) was purchased from EY Laboratories (San Mateo, CA). RPMI 1640 cell medium was purchased from VWR (West Chester, PA). Fetal bovine serum (FBS), penicillin, and streptomycin were purchased from Invitrogen (Carlsbad, CA). Molt-3 T-lymphocyte line was purchased from American Type Culture Collection (ATCC).

2.1.2. Preparation of T-cell binding surfaces

Glass substrates were first modified with 3-acryloxypropyl trichlorosilane to promote antibody adsorption according to previously reported procedures [24,25]. Briefly, glass slides were treated in an oxygen plasma chamber (YES-R3, San Jose, CA) at 300 W for 5 min. The substrates were then incubated in 2 mM solution of 3-acryloxypropyl trichlorosilane diluted in anhydrous toluene for 1 h. Silanized slides were then rinsed in fresh toluene, dried under nitrogen, dehydrated at 100 °C for 2 h, and stored in a desiccator prior to use. To prepare areas for T-cell capture, 0.2 mg/ml purified mouse anti-CD4 antibody dissolved in 1× PBS solution with 0.005% Tween-20 was printed onto silanized glass slides using a Micro-Caster hand-held microarrayer system (Whatman Schleicher and Schuell). Similarly, 10 µg/ml AuNP/anti-CD4 conjugate antibody containing 0.005% Tween-20 was also printed.

2.1.3. Formation of gold nanoparticle labeled cellular micropatterns

Molt-3 cells were maintained in RPMI 1640 media with 10% (v/v) fetal bovine serum (FBS), 100 µg/ml penicillin and 100 µg/ml streptomycin at 37 °C in a humidified atmosphere with 5% CO₂. The cells were spun down at 1200 rpm for 3 min and then suspended in 1× PBS to a final concentration of 5 × 10⁶ cells/ml. The cells were seeded onto anti-CD4 antibody arrayed substrates. After one hour incubation at 37 °C, substrates were washed with 1× PBS solution to remove unattached cells. Substrates with patterned adherent T-cells were then fixed with 4% formalin solution for 15 min followed by three washes in 1× PBS solution. Finally, substrates were incubated with 10 µg/ml AuNP/anti-CD4 conjugate antibody for 1 h followed by washing in 1× PBS to remove unattached gold particles.

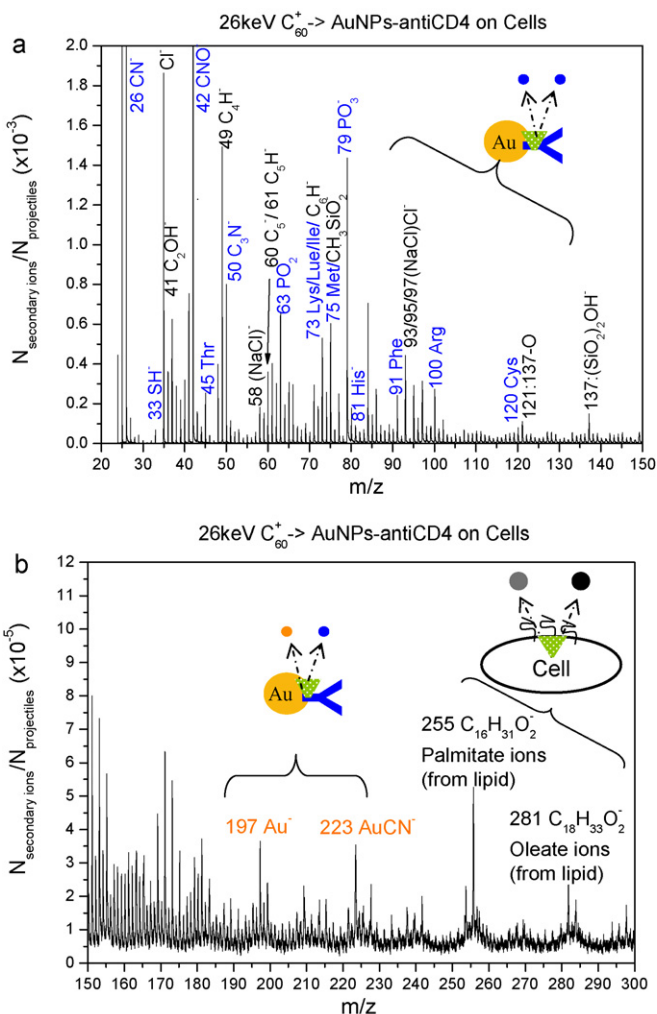


Fig. 1. Secondary ion mass spectrum of AuNPs-antiCD4 on Molt-3 cell micropatterned surfaces analyzed with 26 keV C₆₀⁺ ToF-SIMS. (a) m/z 30–150 and (b) m/z 150–300.

2.2. Instrumentation

2.2.1. ToF-SIMS with the event-by-event bombardment/detection mode

The effusion C₆₀ ToF-SIMS instruments, custom-built in our laboratory, produce C₆₀^{1,2+} projectiles with total impact energy on the target sample of 26 keV and 43 keV for singly and doubly charged C₆₀ ions respectively [26–28]. The gaseous C₆₀ is generated by heating C₆₀ powder placed in a Cu heating reservoir until it sublimates. The effusion vapor of C₆₀ is then electron impact ionized by electrons emitted from a heated tungsten wire or tantalum disk to yield C₆₀^{1,2+} ions. The primary ions are focused with electrostatic lenses and mass selected with a Wien filter. C₆₀^{1,2+} ions are then steered toward an off-center aperture that prevents the neutrals from impacting the negatively biased target. The electrons and negative secondary ions emitted from the target are extracted by a grounded electrode. Electrons are deflected by a weak magnetic field to strike a start detector (start signal). The SIs are detected with a stop detector composed of a micro channel plate (MCP) assembly with an 8-anode detector capable of detecting up to 8 isobaric ions per event [26]. The event-by-event bombardment-detection mode allows to acquire and record the data for each individual projectile impact [29]. The Total Matrix of Events (TME[®]) software is used to acquire and process data in the event-by-event mode. An event is determined by the detection of ejected electron and their simul-

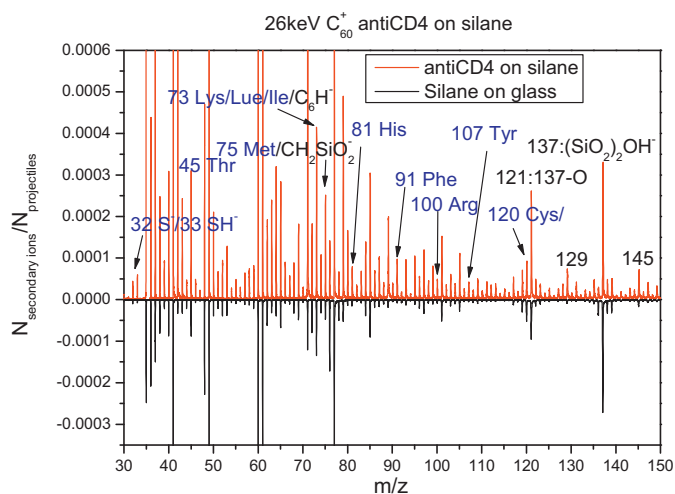


Fig. 2. Secondary ion mass spectra of anti-CD4 on silane glass slide (top) and silane on glass slide (bottom) impacted with 26 keV C_{60}^+ primary ions.

taneously ejected SIs from a single projectile impact resulting in an emission area ~ 10 nm in diameter [30]. The co-emissions of SIs originate from the co-localized molecules within the nanometric volume. The secondary ion mass spectrum is obtained by accumulation of several million impact/emission events, and is similar to a conventional SIMS spectrum. To obtain a coincidental ion mass spectrum, a mass window is set on specific ion of interest. The extracted SIs in the coincidence ion mass spectrum represents the spatially co-located ions.

2.2.2. ToF-SISM analysis

The samples were on glass substrates modified with anti-CD4 Abs and incubated with CD4 antigen-expression T-cell line (Molt-3). Molt-3 cells captured on the glass surfaces were incubated with AuNPs/anti-CD4 conjugates. They were analyzed with a sequence of individual $C_{60}^{1,2+}$ projectiles at total energies of 26 and 43 keV respectively. To obtain statistically valid data, the experiments were run with a total of $\sim 10^6$ single impacts each spaced $\sim 10^{-3}$ s apart, over a sampling area (800 μm diameter) covering ~ 3000 cells. In the conventional secondary ion mass spectrum, antibodies and cell receptors produce similar characteristic peaks. AuNP labeling was used to impart signature mass peaks to antiCD4 molecules. AuNPs generated specific negative Au and Au adduct ions in the secondary ion mass spectrum that allowed to identify the AuNPs–antiCD4 in a complex biological system. We also employed the SEM to visualize the presence of AuNPs (~ 30 nm in diameter) on the cell surfaces.

2.3. SEM

The AuNPs and cells were analyzed by the scanning electron microscope (SEM; Jeol-7500F Cold Field Emission). SEM operated on gentle beam mode (1 kV) was used to image the morphology and shape of cells ($\times 700$ magnification) and AuNPs ($\times 70,000$ magnification) under vacuum ($\sim 10^{-5}$ Torr).

3. Results and discussion

3.1. Secondary ion mass spectrum and SEM images of AuNPs–antiCD4 on cells

The secondary ion mass spectrum of the AuNPs–antiCD4 conjugates immobilized on cells is shown in Fig. 1. Similar to conventional SIMS, the cumulative SIs mass spectrum shows the

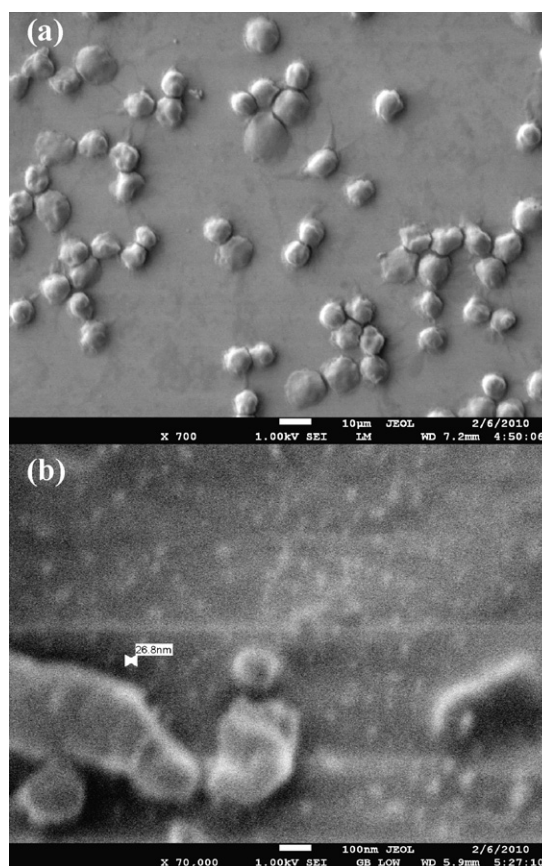


Fig. 3. SEM images of AuNPs–antiCD4 labeled on cell micropatterned surfaces. (a) Molt-3 cells (~ 9 μm in diameter), scale bar: 10 μm and (b) AuNPs–antiCD4 attached on Molt-3 cell, scale bar: 100 nm.

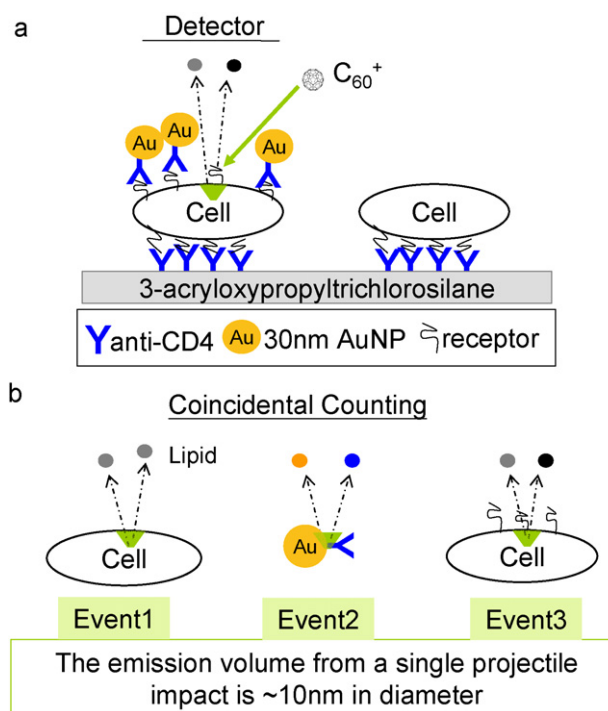


Fig. 4. (a) Schematic illustration of C_{60}^+ impacted on a AuNPs–antiCD4 labeled cell surface and (b) individual events records.

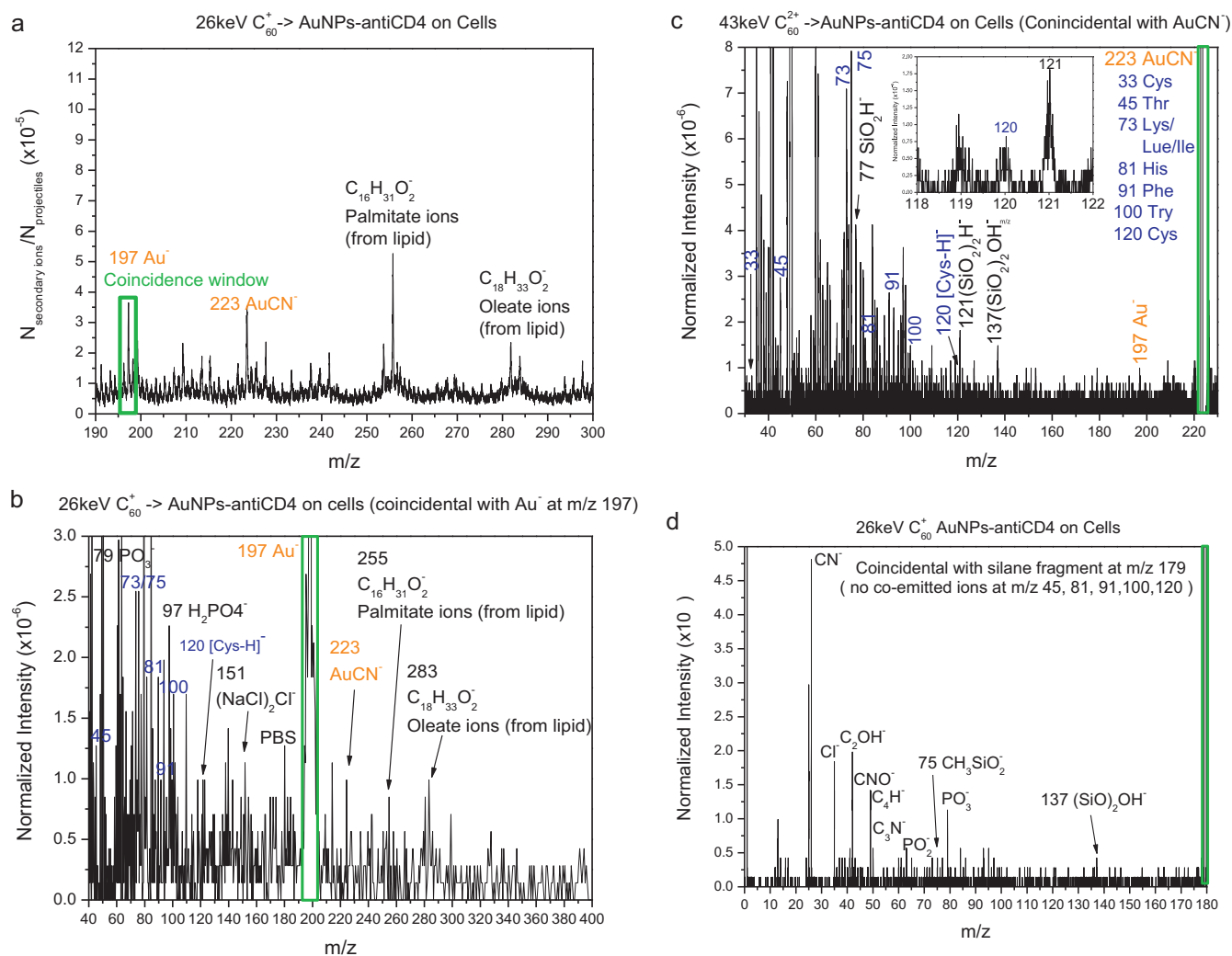


Fig. 5. (a) Original secondary ion mass spectrum of AuNPs-antiCD4 labeled on Molt-3 cells; (b) coincidental ion mass spectrum of co-emitted ions with Au^- (m/z 197); (c) coincidental ion mass spectrum of co-emitted ions with $AuCN^-$ (m/z 223), inserted spectrum represents coincidental intensity of ion at m/z 120; (d) coincidental ion mass spectrum of co-emitted ions with silane fragment at m/z 179.

chemical information of the complex surfaces. The negative ions in the mass range from m/z 30 to 120 are labeled as peaks suggested to originate from amino acid residue side chains, i.e., indicating the presence of antibodies (shown in Fig. 1(a)). A corroborating indication of these peaks arising from amino acids is the increase in their intensities when comparing the immobilized antiCD4 to the silane background (shown in Fig. 2). The palmitate ($C_{16}H_{31}O_2^-$) and oleate ($C_{18}H_{33}O_2^-$) ions originate from the topmost layer of cell surfaces that are composed of the cellular lipid membranes (Fig. 1(b)). The peaks at m/z 197 (Au^-) and 223 ($AuCN^-$) are AuNP adducts emitted from the AuNPs labeled on antibodies (anti-CD4) bound to the cell receptor sites. These unique signals corresponding to AuNPs at m/z 197 (Au^-) and 223 ($AuCN^-$) confirms the successful immobilization of AuNPs-antiCD4 to cells.

The presence of AuNPs immobilized on the cell was also verified with SEM images. As shown in Fig. 3(a), the morphology of Molt-3 cells ($\sim 9 \mu m$ diameter) cultured on microcasted anti-CD4 surfaces ($800 \times 1200 \mu m^2$) were investigated by the SEM [31,32]. The SEM images show that cell morphology remains intact in the vacuum environment ($\sim 10^{-6}$ Torr). Fig. 3(b) shows the attachment of AuNPs with size ~ 30 nm in diameter conjugated with anti-CD4 on the Molt-3 cell surfaces. The blurred image of AuNP-antiCD4 on cells indicates the difficulty in using the SEM to image AuNPs of 30 nm in the cellular environment. The high electron dosage of

the SEM technique causes the AuNP-antiCD4 conjugates to become unstable and decompose [4,18].

3.2. Coincidental ion mass spectra of AuNPs-antiCD4 on cells or silane modified glass

The schematic illustration of applying the event-by-event bombardment/detection mode to probe the cellular surface is shown in Fig. 4(a). The random C_{60} projectiles statistically impact either the cell rich region or the AuNPs-antiCD4 area. As shown in Fig. 4(b), the 1st event illustrates a single C_{60}^+ primary ions impact on the lipid membrane region and the detection of co-emitted SIs from a lipid resolved nanovolume of 5–10 nm in depth and 10 nm in the diameter [10]. The 2nd event expresses the projectiles impact on the co-located AuNPs and antiCD4. The 3rd event shows the SIs were resolved from both antigen and cell lipid membrane area. All individual events are isolated and recorded at time and space that allows one to extract and construct coincidental mass spectrum with events of co-emitted ions with a selected ion [29].

In the secondary ion mass spectrum, the Au adduct $AuCN^-$ at m/z 223, indicates the recombination of ions Au and CN from AuNP-antiCD4 within the impacted nanovolume. Fig. 5(b) and (c) indicates the possibility of identifying amino acids related peaks for the antiCD4 when examining co-emitted ions with Au adducts,

Table 1
The quantitative results of AuNPs–antiCD4 on cell micropatterns.

Detected species	Co-emitted secondary ions	Fractional coverage	Numbers in sampling area
AuNPs–antiCD4 conjugates	Au ⁻ and AuCN ⁻	21%	AuNPs ~ 145 million
Cell lipid membrane	C ₁₆ H ₃₁ O ₂ ⁻ and C ₁₈ H ₃₃ O ₂ ⁻	23%	Cells ~ 3430
Cell	Au + lipid membrane	44%	AuNPs Per Cell ~ 42,274

AuCN⁻ (*m/z* 223) or Au⁻ (*m/z* 197). The co-emissions of Au adducts and amino acid SIs arises from the spatial co-location of antiCD4 and AuNPs. A further examination of co-emitted ions with a silane background peak at *m/z* 179 shows the absence of those amino acids peaks, confirming the specific identities of antiCD4 related ions (shown in Fig. 5(d)). A peak at *m/z* 120 may be due to deprotonated cysteine suggesting the closeness of cysteine and AuNP recalling that the emission volume is $\leq 10^3$ nm³ (shown in Fig. 5(b) and (c)). In addition, the side chains corresponding to characteristic amino acid residues are observed in the coincidental spectra co-emitted with Au⁻. Their proximity suggests that the binding sites for AuNPs on the antiCD4 are the sulfur-terminal cysteine and co-existing amino acid residues.

A similar result was obtained with the test case of AuNPs–antiCD4 deposited on a glass surface. The cumulative secondary ion spectrum and the mass spectrum of the coincidental secondary ions with AuCN⁻ (at *m/z* 223) are shown in Fig. 6(a) and (b). In Fig. 6(a), the negative SI at *m/z* 120 may be attributed again to the deprotonated cysteine. The SIs co-emitted with AuCN⁻ (*m/z* 223) are shown in Fig. 6(b). Ions at *m/z* 30–100 are tentatively

assigned to various amino acid residue side chains of antiCD4. SIs Au⁻ and AuCN⁻ originate from AuNPs. The co-emitted SIs illustrates the feasibility of using coincidence ion mass spectrometry to probe the binding site of complexes conjugates.

3.3. Quantitative analysis of AuNPs–antiCD4 conjugates on cells

To identify the number of complex species on the cell surface we applied a methodology that has been previously described for determining the fractional coverage of immobilized biomolecules on micropatterned surfaces [22]. The fractional coverage is the ratio of the effective number of projectile impacts on a specified sampling area (N_e) to the total number of impacts (N_0) as shown follows: Briefly, two co-emitted ions, A and B originating from the same compound (in the present case from emitted species lipid membrane or AuNPs) have a correlation coefficient, $Q_{A,B}$, of unity. $Q_{A,B}$ is computed as follows:

$$Q_{A,B} = \frac{Y_{A,B}}{Y_A Y_B} = 1 \quad (1)$$

where $Y_{A,B}$ is the coincidental yield of simultaneously detected ions A and B. Y_A and Y_B are the SI yields of detected ions A and B, respectively. The coincidental yield $Y_{A,B}$ is:

$$Y_{A,B} = \frac{I_{A,B}}{N_e} \quad (2)$$

where N_e is the effective number of impacts on a specific specimen and $I_{A,B}$ is the number of co-emitted ions A and B, recorded in the coincidental mass spectrum.

The SI yields of ion A and B are computed as follows:

$$Y_A = \frac{I_A}{N_e} \quad (3)$$

$$Y_B = \frac{I_B}{N_e} \quad (4)$$

where I_A and I_B are the peak areas of ions A and B, respectively. Using Eqs. (1)–(4) one can calculate N_e :

$$N_e = \frac{I_A I_B}{I_{A,B}} \quad (5)$$

For a practical application, we use the coverage coefficient, K , to express the fractional coverage of specimens on the micropatterned surface:

$$K = \frac{N_e}{N_0} \times 100\% \quad (6)$$

As listed in Table 1, we determined the fractional coverage of membrane lipid to be ~23% of the cell micropatterned surface using the co-emitted ions C₁₆H₃₁O₂⁻ and C₁₈H₃₃O₂⁻ from lipids. The fractional coverage of the AuNPs was found to be ~21% based on the co-emitted Au⁻ and AuCN⁻ ions as shown in Fig. 5(b). The AuNP coverage indicates the binding density of AuNPs labeled anti-CD4 on the cell receptor sites. The percentage of each specimen allowed us to calculate their densities in the sampling area. The sampling area is about 800 μm in diameter. Within this area, 21% of the patterned surface is covered with AuNPs–antiCD4 conjugates. It should be noted that the cell surface is partially covered by the 30 nm size AuNPs (Fig. 4(a)), thus the effective impacts on the cell surface were reduced by the presence of AuNPs. Thus to calculate the number of

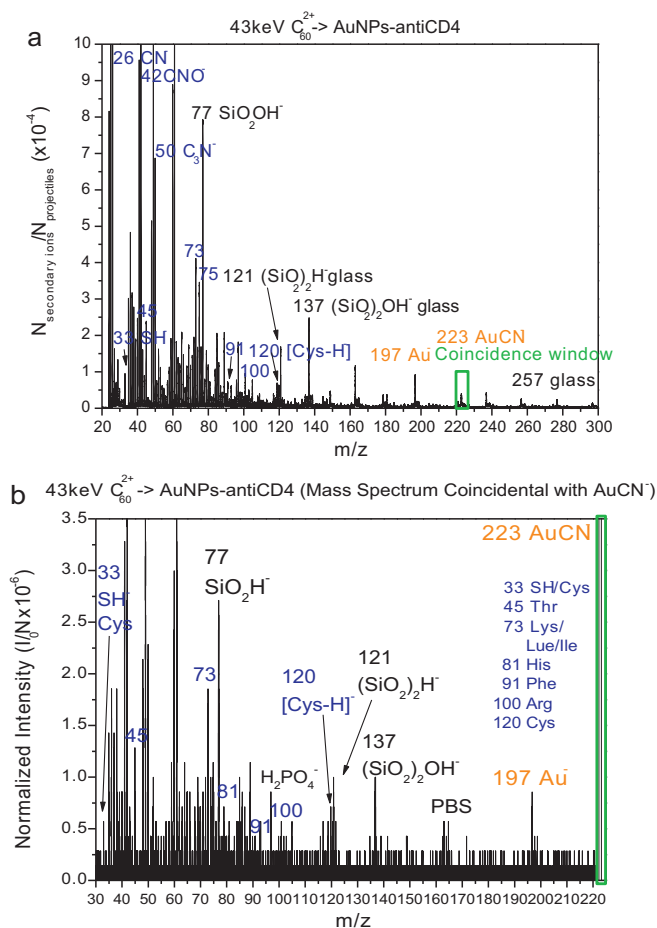


Fig. 6. (a) Secondary ion mass spectrum of AuNPs–antiCD4 on glass impacted with 43 keV C₆₀²⁺ primary ions and (b) coincidental ion mass spectrum of co-emitted ions with AuCN⁻ (*m/z* 223) for AuNPs–antiCD4 on acrylated silane modified glass.

cells within the sampling area, the fractional coverage of AuNPs needed to be taken into account. As a result, the total cell coverage was found to be ~44% of the sampling area. The data corresponding to the number of cells or AuNPs are listed in Table 1. The number of cells in the sampling area was ~3430 while the number of AuNPs was 1.45×10^8 . The resulting number of AuNPs per cell was about 42,274 which is in a good agreement with the literature result measured by flow cytometry [33,34].

4. Conclusions

This study illustrates the ability of SIMS in the individual impact mode to: (a) validate the immobilization of AuNP labeled anti-CD4 on cell surfaces and (b) quantify the coverage of molecules expressed on the cell surface. This method has several promising features for analysis of bio-nanomaterials and cells. Coincidence SIMS may be used to analyze nanoparticles that fall below the detection limit of standard electron microscopy, and should thus be applicable for studies on size dependent binding of nanoparticle–antibody conjugates [20]. As demonstrated by this work, SIMS may also be used to quantify the density of cell surface antigens. Beyond analysis of numbers, SIMS also provide chemical composition of the cell surface molecules and may in the future be used to analyze changes in composition (e.g., mutations) of cell surface receptors. We envision mass spectrometry of cell surfaces to have future applications in cancer research, immunology and the study of infectious diseases.

Acknowledgements

This work was supported by the National Science Foundation (Grant-CHE 0750377 to EAS) and by the National Institutes of Health (Grant-EB 006519 to AR). The scanning electron microscope (SEM) images were taken in the Materials and Characterization Facility in Texas A&M University.

References

- [1] J.F. Hainfeld, F.R. Furuya, A 1.4-Nm gold cluster covalently attached to antibodies improves immunolabeling, *J. Histochem. Cytochem.* 40 (1992) 177–184.
- [2] C.H. Liang, C.C. Wang, Y.C. Lin, C.H. Chen, C.H. Wong, C.Y. Wu, Iron oxide/gold core/shell nanoparticles for ultrasensitive detection of carbohydrate–protein interactions, *Anal. Chem.* 81 (2009) 7750–7756.
- [3] G. Depanfilis, G.C. Manara, C. Ferrari, C. Torresani, Simultaneous colloidal gold immunoelectronmicroscopy labeling of Cd1a Hla-Dr, and Cd4 surface-antigens of human epidermal langerhans cells, *J. Invest. Dermatol.* 91 (1988) 547–552.
- [4] J.F. Hainfeld, A small gold-conjugated antibody label—improved resolution for electron-microscopy, *Science* 236 (1987) 450–453.
- [5] S.T. Wang, K.J. Chen, T.H. Wu, H. Wang, W.Y. Lin, M. Ohashi, P.Y. Chiou, H.R. Tseng, Photothermal effects of supramolecularly assembled gold nanoparticles for the targeted treatment of cancer cells, *Angew. Chem. Int. Ed.* 49 (2010) 3777–3781.
- [6] G. Depanfilis, D. Soligo, G.C. Manara, C. Ferrari, C. Torresani, Adhesion molecules on the plasma-membrane of epidermal-cells. 1. Human resting langerhans cells express 2 members of the adherence-promoting Cd11/Cd18 family, namely, H-Mac-1 (Cd11b/Cd18) and Gp-150,95 (Cd11c/Cd18), *J. Invest. Dermatol.* 93 (1989) 60–69.
- [7] E.C. Cho, Y. Liu, Y.A. Xia, A simple spectroscopic method for differentiating cellular uptakes of gold nanospheres and nanorods from their mixtures, *Angew. Chem. Int. Ed.* 49 (2010) 1976–1980.
- [8] R. Das, R. Jagannathan, C. Sharan, U. Kumar, P. Poddar, Mechanistic study of surface functionalization of enzyme lysozyme synthesized Ag and Au nanoparticles using surface enhanced Raman spectroscopy, *J. Phys. Chem. C* 113 (2009) 21493–21500.
- [9] E.C. Cho, L. Au, Q. Zhang, Y. Xio, The effects of size, shape, and surface functional group of gold nanostructures on their adsorption and internalization by cells, *Small* 6 (2010) 517–522.
- [10] Z. Li, S.V. Verkhoturov, J.E. Locklear, E.A. Schweikert, Secondary ion mass spectrometry with C-60(+) and Au-400(4+) projectiles: depth and nature of secondary ion emission from multilayer assemblies, *Int. J. Mass Spectrom.* 269 (2008) 112–117.
- [11] S.F. Wang, X. Zhang, X. Mao, Q.X. Zeng, H. Xu, Y.H. Lin, W. Chen, G.D. Liu, Electrochemical immunoassay of carcinoembryonic antigen based on a lead sulfide nanoparticle label, *Nanotechnology* 19 (2008).
- [12] H. Wu, G.D. Liu, J. Wang, Y.H. Lin, Quantum-dots based electrochemical immunoassay of interleukin-1 alpha, *Electrochem. Commun.* 9 (2007) 1573–1577.
- [13] J.V. Jokerst, P.N. Floriano, N. Christodoulides, G.W. Simmons, J.T. McDevitt, Integration of semiconductor quantum dots into nano-bio-chip systems for enumeration of CD4+ T cell counts at the point-of-need, *Lab Chip* 8 (2008) 2079–2090.
- [14] C. Hager-Braun, K.B. Tomer, Characterization of the tertiary structure of soluble CD4 bound to glycosylated full-length HIVgp120 by chemical modification of arginine residues and mass spectrometric analysis, *Biochemistry* 41 (2002) 1759–1766.
- [15] B. Crise, J.K. Rose, Identification of palmitoylation sites on cd4, the human-immunodeficiency-virus receptor, *J. Biol. Chem.* 267 (1992) 13593–13597.
- [16] J.H. Wang, Y.W. Yan, T.P.J. Garrett, J.H. Liu, D.W. Rodgers, R.L. Garlick, G.E. Tarr, Y. Husain, E.L. Reinherz, S.C. Harrison, Atomic-structure of a fragment of human Cd4 containing 2 immunoglobulin-like domains, *Nature* 348 (1990) 411–418.
- [17] J.F. Hainfeld, Site-specific cluster labels, *Ultramicroscopy* 46 (1992) 135–144.
- [18] J.F. Hainfeld, C.J. Foley, L.E. Maelia, J.J. Lipka, 11 tungsten atom cluster labels—high-resolution, site-specific probes for electron-microscopy, *J. Histochem. Cytochem.* 38 (1990) 1787–1793.
- [19] T. Schenkel, K.J. Wu, Probing nano-environments of peptide molecules on solid surfaces by highly charged ion secondary ion mass spectrometry, *Int. J. Mass Spectrom.* 229 (2003) 47–53.
- [20] S. Rajagopalachary, S.V. Verkhoturov, E.A. Schweikert, Characterization of individual Ag nanoparticles and their chemical environment, *Anal. Chem.* 81 (2009) 1089–1094.
- [21] S. Rajagopalachary, S.V. Verkhoturov, E.A. Schweikert, Examination of nanoparticles via single large cluster impacts, *Nano Lett.* 8 (2008) 1076–1080.
- [22] L.-J. Chen, S.S. Shah, S.V. Verkhoturov, A. Revzin, E.A. Schweikert, Characterization and quantification of biological micropatterns using cluster-SIMS, *Surf. Interface Anal.* (2010), doi:10.1002/sia.3399.
- [23] H.D. Zhang, P.S. Williams, M. Zborowski, J.J. Chalmers, Binding affinities/avidities of antibody–antigen interactions: quantification and scale-up implications, *Biotechnol. Bioeng.* 95 (2006) 812–829.
- [24] K. Sekine, A. Revzin, R.G. Tompkins, M. Toner, Panning of multiple subsets of leukocytes on antibody-decorated poly(ethylene) glycol-coated glass slides, *J. Immunol. Methods* 313 (2006) 96–109.
- [25] H. Zhu, M. Macal, C.N. Jones, M.D. George, S. Dandekar, A. Revzin, A miniature cytometry platform for capture and characterization of T-lymphocytes from human blood, *Anal. Chim. Acta* 608 (2008) 186–196.
- [26] J.E. Locklear, Secondary ion emission under keV carbon cluster bombardment, Ph.D. Dissertation, Chemistry, Texas A&M University, College Station, TX, 2006.
- [27] S.V. Verkhoturov, M.J. Eller, R.D. Rickman, S. Della-Negra, E.A. Schweikert, Single impacts of C-60 on solids: emission of electrons, ions and prospects for surface mapping, *J. Phys. Chem. C* 114 (2010) 5637–5644.
- [28] M.J. Eller, S.V. Verkhoturov, S. Della-Negra, R.D. Rickman, E.A. Schweikert, Real-time localization of single C60 impacts with correlated secondary ion detection (p n/a), *Surf. Interface Anal.* (2010), doi:10.1002/sia.3400.
- [29] M.A. Park, K.A. Gibson, L. Quinones, E.A. Schweikert, Coincidence counting in time-of-flight mass-spectrometry—a test for chemical microhomogeneity, *Science* 248 (1990) 988–990.
- [30] R.D. Rickman, S.V. Verkhoturov, E.S. Parilis, E.A. Schweikert, Simultaneous ejection of two molecular ions from keV gold atomic and polyatomic projectile impacts, *Phys. Rev. Lett.* 92 (2004) 047601-1–047601-4.
- [31] S.S. Shah, M.C. Howland, L.J. Chen, J. Silangcruz, S.V. Verkhoturov, E.A. Schweikert, A.N. Parikh, A. Revzin, Micropatterning of proteins and mammalian cells on indium tin oxide, *ACS Appl. Mater. Interfaces* 1 (2009) 2592–2601.
- [32] H. Zhu, G. Stybayeva, J. Silangcruz, J. Yan, E. Ramanculov, S. Dandekar, M.D. George, A. Revzin, Detecting cytokine release from single T-cells, *Anal. Chem.* 81 (2009) 8150–8156.
- [33] K.A. Davis, B. Abrams, S.B. Iyer, R.A. Hoffman, J.E. Bishop, Determination of CD4 antigen density on cells: role of antibody valency, avidity, clones, and conjugation, *Cytometry B: Clin. Cytom.* 33 (1998) 197–205.
- [34] L. Wang, F. Abbasi, A.K. Gaigalas, R.A. Hoffman, D. Flagler, G.E. Marti, Discrepancy in measuring CD4 expression on T-lymphocytes using fluorescein conjugates in comparison with unimolar CD4-phycoerythrin conjugates, *Cytometry* 72B (2007) 442–449.